Original Paper

TGF-β Type I Receptor Kinase Inhibitor EW-7197 Suppresses Cholestatic Liver Fibrosis by Inhibiting HIF1α-Induced Epithelial Mesenchymal Transition

Min-Jin Kim[a]   Sang-A Park[a]   Chun Hwa Kim[b]   So-Yeon Park[a]   Jung-Shin Kim[a]
Dae-Kee Kim[a]   Jeong-Seok Nam[c]   Yhun Yhong Sheen[a]

[a]College of Pharmacy, Ewha Womans University, Seoul, [b]New Drug Discovery Lab, Hyundai Pharm, Yongin, [c]Laboratory of Tumor Suppressor, Lee Gil Ya Cancer and Diabetes Institute, Gachon University, Incheon, Korea

Abstract
Background/Aims: Hypoxia is an environmental factor that aggravates liver fibrosis. HIF1α activates hepatic stellate cells (HSCs) and increases transforming growth factor-β (TGF-β) signaling and the epithelial mesenchymal transition (EMT), accelerating the progression of fibrosis. We evaluated the anti-fibrotic therapeutic potential of a small-molecule inhibitor of TGF-β type I receptor kinase, EW-7197, on HIF1α-derived TGF-β signaling in cholestatic liver fibrosis. ***Methods:*** We used a bile duct ligation (BDL)-operated rat model to characterize the role of HIF1α-derived TGF-β signaling in liver fibrosis. Cellular assays were performed in LX-2 cells (human immortalized HSCs). The anti-fibrotic effects of EW-7197 in liver tissues and HSCs were investigated via biochemical assays, immunohistochemistry (IHC), immunofluorescence (IF), chromatin immunoprecipitation (ChIP) assays, real-time PCR, and western blotting. ***Results:*** In our BDL rat model, orally administered EW-7197 inhibited fibrosis and attenuated HIF1α-induced activation of HSCs and EMT *in vivo*. In addition, EW-7197 inhibited HIF1α-derived HSC activation and expression of EMT markers in LX-2 cells *in vitro*. ***Conclusion:*** This study suggests that EW-7197 exhibits potential as a treatment for liver fibrosis because it inhibits HIF1α-induced TGF-β signaling.

© 2016 The Author(s)
Published by S. Karger AG, Basel

Introduction

Hepatic fibrosis is caused by various types of chronic liver injury. Fibrosis is characterized by enhanced accumulation of extracellular matrix (ECM) proteins, such as collagen (Col1a) and fibronectin [1]. In response to injury, hepatic stellate cells (HSCs) are activated into myofibroblasts and become a major source of ECM proteins [2-4]. In addition, the epithelial

Yhun Y. Sheen, Ph.D.

College of Pharmacy, Ewha Womans University, Seodaemun-gu, Seoul, 120-750, (Korea)
Tel. +82-2-3277-3028, Fax +82-2-3277-2851, E-Mail yysheen@ewha.ac.kr

KARGER

mesenchymal transition (EMT) has been identified as an important mechanism in fibrotic progression [5]. Although recent studies have demonstrated that numerous mediators are essential for the initiation and progression of fibrosis, the association among these mediators remains unclear. Various studies have demonstrated that chemical and surgical liver injuries cause hypoxia in the liver [6-9]. Disruption of hepatic blood flow causes hypoxia, leading to deposition of ECM proteins [9, 10]. Hypoxia aggravates inflammation through generation of reactive oxygen species (ROS) [11], which might bring about the EMT [12]. Hypoxia may activate various transcription factors, such as hypoxia-inducible factor 1α (HIF1α) and vascular endothelial growth factor (VEGF) in order to regulate gene expression and cellular signaling [13]. HIF1α modulates the EMT in several cell lines; HIF1α-induced EMT is involved in cancer progression, metastasis, and organ fibrosis [14-17]. In addition, transforming growth factor-β (TGF-β) signal transduction might play a pivotal role in HSC activation by HIF1α [18, 19]. TGF-β is a fibrogenic mediator involved in activation and transdifferentiation of HSCs [20, 21]. TGF-β acts via canonical and non-canonical signaling pathways. Canonically, TGF-β binding to the TGF-β type II receptor (TβRII), recruits the TGF-β type I receptor (TβRI), and activates a TβRI kinase such as a activin-like kinase 5 (ALK5). ALK5 phosphorylates receptor-associated Smad2/3, after which p-Smad2/3 interacts with Smad4 to transactivate target genes [22]. Smad-dependent canonical TGF-β signaling plays a critical role in HSC activation and EMT progression during liver fibrosis [23-26]. Therefore, canonical TGF-β signal plays a central role in the molecular pathogenesis of liver fibrosis and might serve as a potential target for treatments for patients with hepatic fibrosis [27]. Recently, synthetic inhibitors of TGF-β have been reported to suppress hepatic fibrosis in experimental animal models [28, 29].

We previously reported that a novel small-molecule inhibitor of ALK5, EW-7197, inhibited fibrosis in the liver, kidneys, and lungs by inhibiting TGF-β/Smad and ROS signaling [29]. In this study, we investigated the anti-fibrotic effect of EW-7197 (20 and 40 mg/kg) in bile duct-ligated (BDL) rats and showed that the higher dose of EW-7197 inhibited fibrosis by inhibiting HIF1α-induced EMT.

Materials and Methods

Reagents

EW-7197, LY2157299, and IN-2001 were provided by Dr. D.K. Kim (Ewha Womans University, Seoul, Republic of Korea). Recombinant human TGF-β1 was purchased from R&D Systems (Minneapolis, MN, USA), and $CoCl_2$ was purchased from Sigma-Aldrich (St. Louis, MO, USA). Glucose oxidase (GOX) was obtained from Dr. H.A. Woo (Ewha Womans University).

Cell lines and culture

LX-2 immortalized human HSCs were maintained in Dulbecco's modified Eagle medium (DMEM) containing 10% fetal bovine serum. All of the media were purchased from Invitrogen (Carlsbad, CA, USA). The cells were maintained at 37°C in a humidified incubator in the presence of 5% CO_2.

Experimental design for cholestatic liver fibrosis models

Six-week-old male Sprague-Dawley (SD) rats were purchased from Orient Bio, Inc. (Seoul, Republic of Korea). SD rats weighing 180 to 200 g were randomly divided into five experimental groups: sham-operated rats (sham rats) as controls (n = 5); sham rats treated with 40 mg/kg EW-7197 (n = 5); BDL-operated rats (BDL rats) (n = 10); BDL rats treated with 20 mg/kg EW-7197 (n = 10); and BDL rats treated with 40 mg/kg EW-7197 (n = 10). For BDL, the animals were anesthetized with Zoletil (20 mg/kg) and xylazine (10 mg/kg), after which the common bile duct was exposed and double-ligated using 4-0 silk sutures. The first ligature was placed below the junction of the hepatic ducts, whereas the second ligature was placed above the entrance of the pancreatic ducts. For the sham-operated rats, an incision was made in the abdomen and then closed without any further surgical procedure (Fig. 1A). The animals were maintained in a temperature-controlled room (21°C) and were supplied with autoclaved food and water. At 48 h after the last dosing, the

Cellular Physiology and Biochemistry

Cell Physiol Biochem 2016;38:571-588

DOI: 10.1159/000438651
Published online: February 05, 2016

© 2016 The Author(s). Published by S. Karger AG, Basel
www.karger.com/cpb

573

Kim et al.: EW-7197 Suppresses Cholestatic Liver Fibrosis

animals were sacrificed, after which serum, spleens, and the livers were removed. The livers were sliced into several parts, snap-frozen in liquid nitrogen, and maintained at -70°C. A portion of each liver was immersed in 10% neutral-buffered formalin for histopathological and immunohistochemical examinations. Body weight was measured weekly. In all animals used, body weight, wet liver and spleen weight, and the ratio of
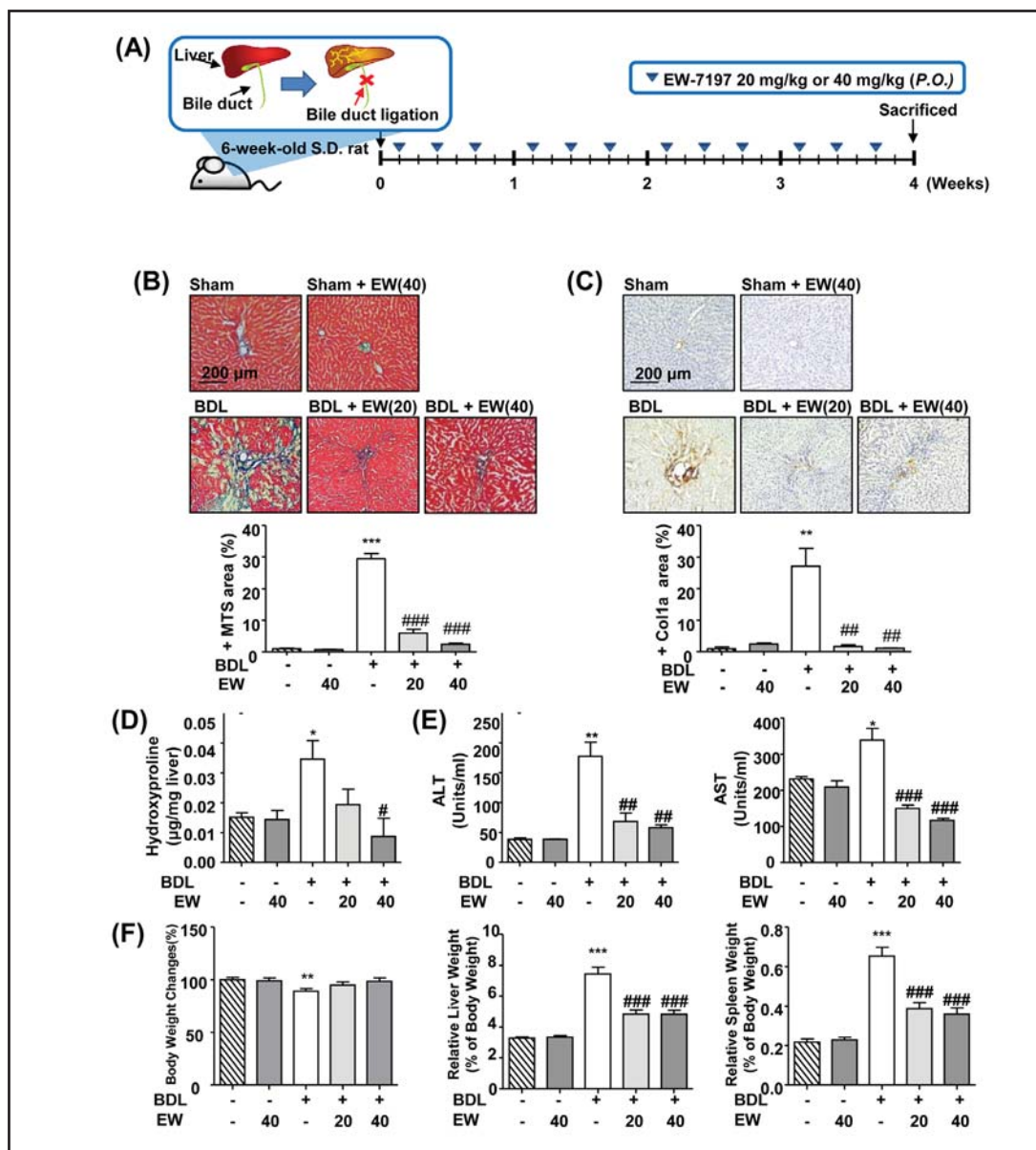

Fig. 1. EW-7197 suppresses BDL-induced liver fibrosis. (A) Scheme of drug treatment. Six-week-old male SD rats were randomly divided into five experimental groups. Twenty-four hours after the BDL or sham operation, EW-7197 (EW: 20 or 40 mg/kg, *qod*) dissolved in vehicle (Veh) was administered to rats orally. EW was administered thrice weekly for 4 weeks. (B) Representative staining (top) and densitometric analysis (bottom) of Masson's trichrome staining of liver tissue from BDL rats. (C) IHC of Col1a (top) and densitometric analysis (bottom) of Col1a staining in liver tissue from BDL rats. (D) Hydroxyproline content in liver tissue from BDL rats was determined by hydroxyproline assay. (E) ALT and AST serum levels. AST and ALT serum levels of BDL rats were determined by enzyme-linked immunosorbent assay (ELISA). EW-7197 (EW: 20, 40 mg/kg, *qod*) dissolved in vehicle (Veh) was administered to rats orally thrice weekly for 4 weeks following BDL. (F) Effects of EW-7197 on body weight changes and relative liver and spleen weight. $*p < 0.05$ vs. sham, $**p < 0.01$ vs. sham, $***p < 0.001$ vs. sham, $#p < 0.05$ vs. BDL, $##p < 0.01$ vs. BDL, $###p < 0.001$ vs. BDL.

liver and spleen weight to body weight were determined. Changes in body weight were calculated as follows.

$$Body\ weight\ changes\ (\%) = \frac{Weight\ at\ 4th\ week - Weight\ at\ 1st\ week}{Weight\ at\ 4th\ week} \times 100$$

(the weight of animals subjected to the sham operation was considered as 100%)

The experimental protocol was approved by The Institutional Animal Care and Use Committee (IACUC) of Ewha Womans University and complied with the NIH Guide for the Care and Use of Laboratory Animals (Institute of Laboratory Animal Resources, National Research Council, WA, USA).

HSC-enriched cell preparation by collagen perfusion methods

Six-week-old male ICR mice were purchased from Orient Bio, Inc. (Seoul, Republic of Korea). HSC-enriched cells and primary hepatocytes were isolated from the livers of 6- to 7-week-old male mice weighing 20 – 25 g. Mouse primary hepatocytes and HSC-enriched cells were isolated by differential centrifugation at $1500 \times g$ to collect HSC-enriched cells after gathering of hepatocytes via centrifugation at $500 \times g$ for 5 min. Each liver was perfused with PBS using a non-circulating system for 10 min at 37°C (2.2 mL/min), followed by perfusion with a perfusion solution consisting of 0.03% (w/v) collagenase (Sigma-Aldrich) in PBS (pH 7.4) with 0.015 % (w/v) $CaCl_2 \cdot 2H_2O$ for 15 to 20 min. Perfusion solution was then circulated through each liver for 15 min to wash the tissue, after which each liver was cut into pieces in ice-cold MEM medium supplemented with 10% FBS and insulin (4 µg/mL). The resulting suspension was filtered through nylon mesh and centrifuged at $400 \times g$ for 5 min. The collected cells were plated onto collagen-coated plates at a density of 5×10^5 cells/mL of culture medium. Serum starvation was performed for 24 h, followed by stimulation with TGF-β1 (2 ng/mL) and treatment with 0.5 µM EW-7197 and 0.5 µM pirfenidone for 24 h.

Proliferation assay

Cell proliferation was measured using a Cell Counting Kit-8 (CCK-8) assay kit (Dojindo Laboratories, Kumamoto, Japan). Cells were seeded on 96-well plates at a density of 5×10^3 cells per well, after which they were treated with 10 nM to 10 µM EW-7197 for 72 h. Next, CCK-8 solution (10 µL) was added to each well, after which the wells were incubated for 1 h at 37°C. Absorbance was measured at 450 nm with an ELISA microplate reader (Versa Max; Molecular Devices, Sunnyvale, CA, USA).

Luciferase Reporter Gene Assay

HaCaT (3TP-Lux stable) cells were seeded on 96-well plates and treated with the indicated concentrations of activin receptor-like kinase 5 (ALK5) inhibitors in the presence or absence of TGF-β (2 ng/mL) for 24 h. Luminescence was measured in cell lysates with a luminometer (Micro Lumat Plus; Berthold Technologies Berthold Technologies, BadWildbad, Germany).

Determination of intracellular ROS generation

Intracellular ROS production was measured using 2′, 7′-dichlorodihydrofluorescein diacetate (H_2DCF-DA) as described below. H_2DCF-DA is a lipid-permeable, nonfluorescent compound that is oxidized by intracellular ROS to form the lipid-impermeable and fluorescent compound dichlorodihydrofluorescein (DCF). Cells were plated at density of 5×10^3 cells per well in 96-well plates (SPL, Pocheon, Korea). H_2DCF-DA was added directly to the culture medium at a final concentration of 10 µM, after which the cells were cultured under standard conditions. ROS arbitrary units were measured using fluorescence microplate reader (BIO-TEK, Winooski, USA) with an excitation wavelength of 485 nm and an emission wavelength of 530 nm. Upon the same cells, protein concentrations were determined using fluorescamine. The results of these experiments were expressed as arbitrary absorbance units/mg protein.

Histopathological examination

Tissues (approximately 9×9 mm sections from the left and caudate lobes of the liver) were fixed and stained using hematoxylin and eosin. Masson's trichrome staining for collagen was used to quantify the fibrotic area. For immunohistochemical analysis, deparaffinized sections were incubated with primary/secondary antibodies. The sections were counterstained with diluted hematoxylin for immunohistochemistry or with 4′, 6-diamidino-2-phenylindole (DAPI) for immunofluorescent staining.

Cellular Physiology and Biochemistry

Cell Physiol Biochem 2016;38:571-588

DOI: 10.1159/000438651
Published online: February 05, 2016

© 2016 The Author(s). Published by S. Karger AG, Basel
www.karger.com/cpb

575

Kim et al.: EW-7197 Suppresses Cholestatic Liver Fibrosis

Immunofluorescence

Cells and animal tissue samples fixed with 4% paraformaldehyde solution (pH 7.4) were blocked in 5% bovine serum albumin with normal serum in 0.1% Triton X-100 and subsequently incubated with primary/ secondary antibodies. The nuclei of the cells were stained with DAPI solution (blue). Images were obtained using an LSM 510 META laser confocal microscopy system (Carl Zeiss, Oberkochen, Germany) at 400 × magnification.

Biochemical assays

The hydroxyproline content of the tissue samples was quantified colorimetrically using the chloramine T method as described by Bergheim et al. [30]. Serum alanine aminotransferase (ALT) and aspartate aminotransferase (AST) activity levels were determined using a spectrophotometric enzyme assay kit (Asan Pharm. Co., Hwaseong, Republic of Korea) according to the manufacturer's instructions.

RNA isolation and reverse-transcriptase polymerase chain reaction (RT-PCR) analyses

Total RNA from tissue samples (sections of approximately 5 × 5 mm from the right lobe of the liver) and cells were

Table 1. Primer sequences

	Species		Sequence (5'→3')
α-sma	Rat	Sense	5'-GTGATCACCATCGGGAATGA-3'
		Antisense	5'-CAGCAATGCCTGGGTACATG-3'
Col-1a1	Rat	Sense	5'-GTGATCACCATCGGGAATGA-3'
		Antisense	5'-CAGCAATGCCTGGGTACATG-3'
CTGF	Rat	Sense	5'-AAGACCTGTGGGATGGGC-3'
		Antisense	5'-TGGTGCAGCCAGAAAGCTC-3'
E-cadherin	Rat	Sense	5'-AACGAGGGCATTCTGAAAACA-3'
		Antisense	5'-CACTGTCACGTGCAGAATGTACTG-3'
Fn	Rat	Sense	5'-GCTTCAAGCTGGGTGTACGA-3'
		Antisense	5'-AAGTTGGTTGGGGGAGACAG-3'
β-actin	Rat	Sense	5'-AGCCATGTACGTAGCCATCC-3'
		Antisense	5'-TCTCAGCTGTGGTGGTGAAG-3'
Pai-1	Rat	Sense	5'-CCTCATCCTGGGCCTGGTTCTGGTCT-3'
		Antisense	5'-GGTTTTCCCCGCTGTGGTCATCTGC-3'
Tgf-β1	Rat	Sense	5'-AATATAGCAACAATTCCTGGCGTTA -3'
		Antisense	5'-CTGCCGGACAACTCCAGTGA -3'
Snai1	Rat	Sense	5'-ACCACTATGCCGCGCTCTT -3'
		Antisense	5'-GGTCGTAGGGCTGCTGGAA -3'
α-SMA	Human	Sense	5'-CATCATGCGTCTGGATCTGG-3'
		Antisense	5'-GGACAATCTCACGCTCAGCA-3'
COL-1A1	Human	Sense	5'-TCTGGAGAGGCTGGTACTGC-3'
		Antisense	5'-GAGCACCAAGAAGACCCTGA-3'
E-CADHERIN	Human	Sense	5'-TCCATTTCTTGGTCTACGCC-3'
		Antisense	5'-CACCTTCAGCCATCCTGTTT-3'
N-CADHERIN	Human	Sense	5'-GTGCCATTAGCCAAGGGAATTCAGC-3'
		Antisense	5'-GCGTTCCTGTTCCACTCATAGGAGG-3'
VIMENTIN	Human	Sense	5'-ACCCGCACCAACGAGAAGGT-3'
		Antisense	5'-ATTCTGCTGCTCCAGGAAGCG-3'
PAI-1	Human	Sense	5'-CCGGAACGACCTGAAGAAGTG-3'
		Antisense	5'-GTGTTTCAGCAGGTGGCGC-3'
PPIA	Human	Sense	5'-TGCCATCGCCAAGGAGTAG-3'
		Antisense	5'-TGCACAGACGGTCACTCAAA-3'
TGF-β1	Human	Sense	5'-AAGGACCTCGGCTGGAAGTG-3'
		Antisense	5'-CCGGGTTATGCTGGTTGTA-3'
SNAIL	Human	Sense	5'-ATCGGAAGCCTAACTACAGC -3'
		Antisense	5'-CAGAGTCCCAGATGAGCATT -3'

isolated using TRIzol reagent (Invitrogen). cDNA was synthesized from 2 μg of total RNA by M-MLV reverse transcriptase (Invitrogen) and random primers (Invitrogen), after which it was subjected to PCR amplification using Taq polymerase (Promega). For real-time quantitative RT-PCR, Power SYBR Green PCR Master Mix and a Step-One Real-time PCR system (Applied Biosystems) were used to amplify the isolated cDNA. The primers used for real-time quantitative RT-PCR are listed in Table 1.

Western blot analysis

Tissue samples (sections of approximately 5 × 5 mm from the right lobe of the liver) and cells were lysed and separated by 6 to 12% sodium dodecyl sulfate-polyacrylamide gel electrophoresis (SDS-PAGE), after which their constituent proteins were transferred to polyvinylidene difluoride (PVDF) membranes. The antibodies used for western blotting are listed in Table 2. The primary antibodies were incubated with each PVDF membrane followed by incubation with appropriate peroxidase-conjugated second antibodies and detection using an enhanced chemiluminescence (ECL) kit. Band intensities were analyzed using a LAS-3000 densitometer (Fujifilm, Tokyo, Japan).

KARGER

Chromatin immunoprecipitation (ChIP) assays

LX-2 cells were treated with EW-7197 or LY2157299 (or IN-2001) in the absence or presence TGF-β (or CoCl$_2$) for 3 h. Cells were harvested and subjected to ChIP assays with anti-Smad2/3 (or anti-HIF1α) at the promoter region upstream of the human PAI-1 gene. The promoter sequence of PAI-1 is provided in Table 3.

Statistical analysis

The results are expressed as the mean ± standard error of the mean (SEM) or as the mean ± standard deviation (SD). Statistical comparisons were conducted using Student's t-test or one-way analysis of variance (ANOVA), followed by Dunnett's two-tailed post-hoc test (SPSS version 10.0; IBM Corporation, Armonk, NY, USA). Results with p-values less than 0.05 were considered statistically significant.

Results

EW-7197 suppresses BDL-induced liver fibrosis

Previously we reported that ALK5 inhibitor EW-7197 strongly

Table 2. Antibody list for Western blot, IHC, IF, and ChIP assay

Antibody	Company	Cat. #
Anti-α-SMA	Sigma	A2547
Anti-β-actin	Sigma	A5316
Anti-CAIX	Milipore	ABC272
Anti-CTGF	Santa Cruz Biotechnology	sc-14939
Anti-COL-1	Santa Cruz Biotechnology	sc-59772
Anti-E-cadherin	BD biosciences	610182
Anti-Fibronectin	BD biosciences	610077
Anti-GAPDH	Cell signaling	5174
Anti-GLUT1	Abcam	ab652
Anti-HIF1α	Abcam	ab113642
Anti-Snail	Cell Signaling	C15D3
Anti-p-Smad2/3	Santa Cruz Biotechnology	sc-11769
Anti-p-Smad3	Cell signaling	9520
Anti-Smad2/3	BD biosciences	610842
Anti-Smad3	Ab frontier	AF9F7
Anti-N-cadherin	BD biosciences	610921
Anti-Vimentin	Abcam	550513

Table 3. PAI-1 promoter sequence

ChIP assay	Species		Sequence (5'→3')
PAI-1 promoter	Human	Sense	5'-CCTCCAACCTCAGCCAGACAAG-3'
		Antisense	5'-CCCAGCCCAACAGCCACA-3'

reduced fibrosis in various animal models and organs, including the liver, lung, and kidney, at a low dose (0.625 – 5.0 mg/kg) [29]. In this study, we assessed the anti-fibrotic effects of treatment with 20 and 40 mg/kg EW-7197 every other day in BDL rats, with the aim of examining the effects of higher doses of EW-7197 *in vivo* in order to ensure that such doses have efficacy similar to that of low doses of the drug. In other words, our goal was to confirm that EW-7197 showed a conventional dose-response effect rather than hormesis. Protein kinase and cellular reporter gene assays indicated that the high doses (20 – 40mg/kg) of EW-7197 used in this study specifically inhibited ALK5 [31]. Moreover, a previous study found that a daily dose of 5 to 120 mg/kg EW-7197 for 4 weeks in normal SD rats produced no toxic effects [29]. We investigated the inhibitory effect of EW-7197 on BDL-induced ECM accumulation. Because liver fibrosis is characterized by excessive deposition of ECM proteins, we assessed the collagen content of the livers of BDL rats using various methods. First, we conducted histopathological analysis with Masson's trichrome staining, which stains collagen fibers blue. Staining of collagen fibers around the portal triad in the livers of BDL rats was increased 29-fold in comparison with that of sham rats. Treatment of BDL rats with 20 and 40 mg/kg EW-7197 significantly inhibited collagen accumulation in the liver by 20.43% and 8.25%, respectively, in comparison with that of untreated BDL rats (Fig. 1B). Additionally, immunohistochemistry (IHC) was performed to examine Col1a expression in the livers of BDL rats. Col1a expression in BDL rat livers was increased 27-fold in comparison with that of sham rats. Treatment with 20 or 40 mg/kg EW-7197 decreased Col1a expression in the livers of BDL rats (Fig. 1C). Furthermore, the total amount of collagen in the liver was determined by measuring the amount of hydroxyproline, a major component of collagen protein. The hydroxyproline content of the livers of BDL rats was increased 2.74-

Cellular Physiology and Biochemistry

Cell Physiol Biochem 2016;38:571-588

DOI: 10.1159/000438651
Published online: February 05, 2016

© 2016 The Author(s). Published by S. Karger AG, Basel
www.karger.com/cpb

577

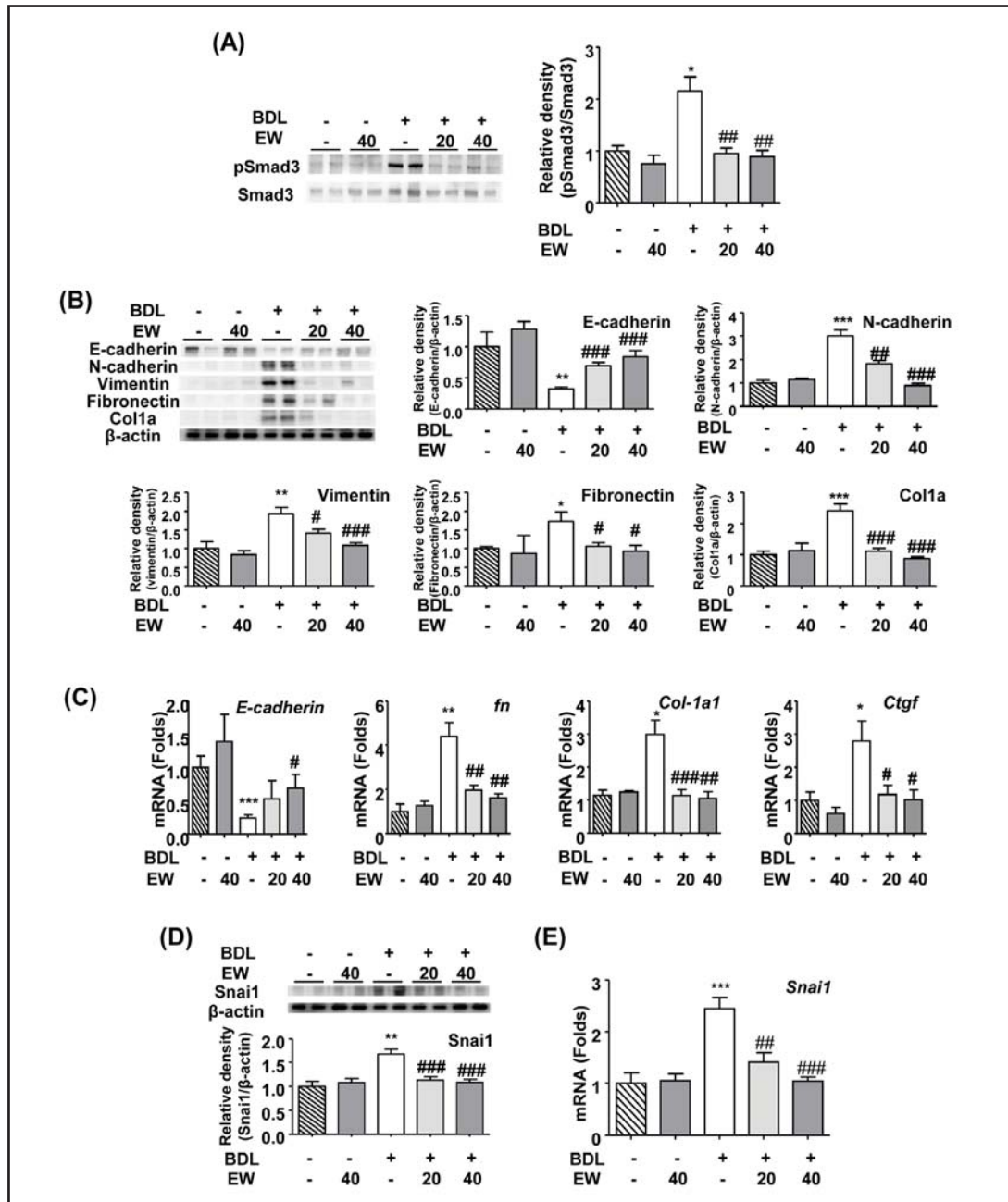Kim et al.: EW-7197 Suppresses Cholestatic Liver Fibrosis

Fig. 2. EW-7197 attenuated the EMT in BDL rats. (A) Effects of EW-7197 on suppression of Smad3 phosphorylation in BDL rat livers. *$p < 0.05$ vs. sham, ##$p < 0.01$ vs. BDL. (B) Effects of EW-7197 on E-cadherin, N-cadherin, vimentin, fibronectin, and Col1a protein expression in BDL rat livers. β-Actin was used as a reference. *$p < 0.05$ vs. sham, **$p < 0.01$ vs. sham, ***$p < 0.001$ vs. sham, #$p < 0.05$ vs. BDL, ##$p < 0.01$ vs. BDL, ###$p < 0.001$ vs. BDL. (C) Effects of EW-7197 on E-cadherin (*E-cadherin*), fibronectin (*Fn*), collagen type 1 (*Col-1a1*), and CTGF (*Ctgf*) mRNA levels in liver tissue from BDL rats. *β-Actin* was used as a reference. *$p < 0.05$ vs. sham, **$p < 0.01$ vs. sham, ***$p < 0.001$ vs. sham, #$p < 0.05$ vs. BDL, ##$p < 0.01$ vs. BDL, ###$p < 0.001$ vs. BDL. (D) Effects of EW-7197 on Snai1 protein expression in BDL rat livers. **$p < 0.01$ vs. sham and ###$p < 0.001$ vs. BDL. (E) *Snai1* mRNA levels in BDL rats were downregulated by EW-7197. *β-Actin* was used as a reference. ***$p < 0.001$ vs. sham, ##$p < 0.01$ vs. BDL and ###$p < 0.001$ vs. BDL.

fold in comparison with that of sham rats. Treatment of BDL rats with 20 and 40 mg/kg EW-7197 reduced hydroxyproline content by 55.94% and 25.41%, respectively, in comparison

Kim et al.: EW-7197 Suppresses Cholestatic Liver Fibrosis

with that of untreated BDL rats (Fig. 1D). These results suggest that EW-7197 inhibited BDL-induced accumulation of collagen *in vivo*. Therefore, we examined the effects of EW-7197 on liver function by monitoring serum ALT and AST levels. The serum ALT and AST levels of BDL rats significantly increased in comparison with those of sham rats. Treatment of BDL rats with 20 mg/kg EW-7197 markedly decreased serum ALT and AST levels by 61.47% and 67.18%, respectively, in comparison with those of untreated BDL rats (Fig. 1E). Treatment of BDL rats with 40 mg/kg EW-7197 markedly decreased serum ALT and AST levels by 44.14% and 35.75%, respectively, in comparison with those of untreated BDL rats (Fig. 1F). The BDL rats exhibited a 10.95% loss of body weight in comparison with that of the sham rats. Additionally, the relative weights of the livers and spleens of the BDL rats were increased 2.26-fold and 3-fold, respectively, in comparison with those of the sham rats. Although EW-7197 did not affect the body weight or organ weight of healthy rats, EW-7197 attenuated BDL-induced changes in body weight and the relative weights of the liver and spleen (Fig. 1G). These data show that EW-7197 suppressed liver fibrosis and improved liver function in BDL rats without toxicity.

EW-7197 attenuated the EMT in BDL rats

To investigate the effects of EW-7197 on TGF-β signaling related to liver fibrosis, we assessed Smad3 phosphorylation in the livers of BDL rats. Smad3 phosphorylation was increased 2.15-fold in the livers of BDL rats in comparison with that of sham rats. EW-7197 inhibited Smad3 phosphorylation in the livers of BDL rats (Fig. 2A). The EMT plays a central role in the development of fibrosis [23, 25, 32]. To examine the effects of EW-7197 on the EMT in BDL rats, we measured the expression of EMT markers. As shown in Fig. 2B, EW-7197 restored expression of the epithelial marker E-cadherin, which was not evident in the livers of BDL rats. EW-7197 reduced the elevated protein levels of mesenchymal markers such as N-cadherin, vimentin, fibronectin, and Col1a in the livers of BDL rats (Fig. 2B). Furthermore, EW-7197 attenuated the decrease in E-cadherin mRNA level and increase in fibronectin, Col1a, and CTGF mRNA levels observed in the livers of BDL rats (Fig. 2C). These results show that EW-7197 inhibits the EMT in the livers of BDL rats. Snail is a master regulator of the EMT that plays an essential role in tumor metastasis [33, 34], but its role in liver fibrosis is unclear. Snail expression was elevated in the livers of BDL rats at the protein (Fig. 2D) and mRNA levels (Fig. 2E); however, BDL rats treated with EW-7197 showed decreased protein and mRNA levels of Snail in comparison with those of untreated BDL rats. These results suggest that EW-7197 inhibits Snail-mediated EMT during BDL-induced fibrogenesis.

EW-7197 inhibits HSC activation

The pathogenesis of fibrosis involves various cell types in the liver, including hepatocytes, Kupffer cells, sinusoidal endothelial cells, and HSCs. Although numerous cytokines and signaling pathways are involved in the progression of liver fibrosis, hypoxia and TGF-β drive injury-induced fibrosis by mediating injury-induced inflammation and contributing to hepatocyte apoptosis [35] and activation of quiescent HSCs [1, 32]. HSC activation and transformation into myofibroblasts play a key role in the progression of liver fibrosis, which is accompanied by elevated expression of α-SMA [1, 36, 37]. As shown in Fig. 3A, IHC staining showed dramatic accumulation of α-SMA-positive cells around the portal triad of the livers of BDL rats; however, EW-7197 treatment decreased α-SMA-positive cell accumulation. In accordance with the IHC results, EW-7197 also decreased the elevated protein and mRNA levels of α-SMA in the livers of BDL rats (Fig. 3B and 3C). These results indicate that TGF-β is a strong driver of HSC activation in BDL-induced liver fibrosis and demonstrate that EW-7197 efficiently inhibits such activation *in vivo*. Because TGF-β induces the EMT in certain pathogenic situations, we tested whether HSCs and hepatocytes were involved in TGF-β-induced EMT. Therefore, we conducted *in vitro* experiments using mouse HSC-enriched cells and primary mouse hepatocytes. EW-7197 did not show cytotoxic effects in HSC-enriched cells, hepatocytes, or LX-2 cells (Fig. 3D). Mouse HSC-enriched cells showed dramatic changes in expression levels of EMT markers E-cadherin, N-cadherin, and vimentin (Fig.
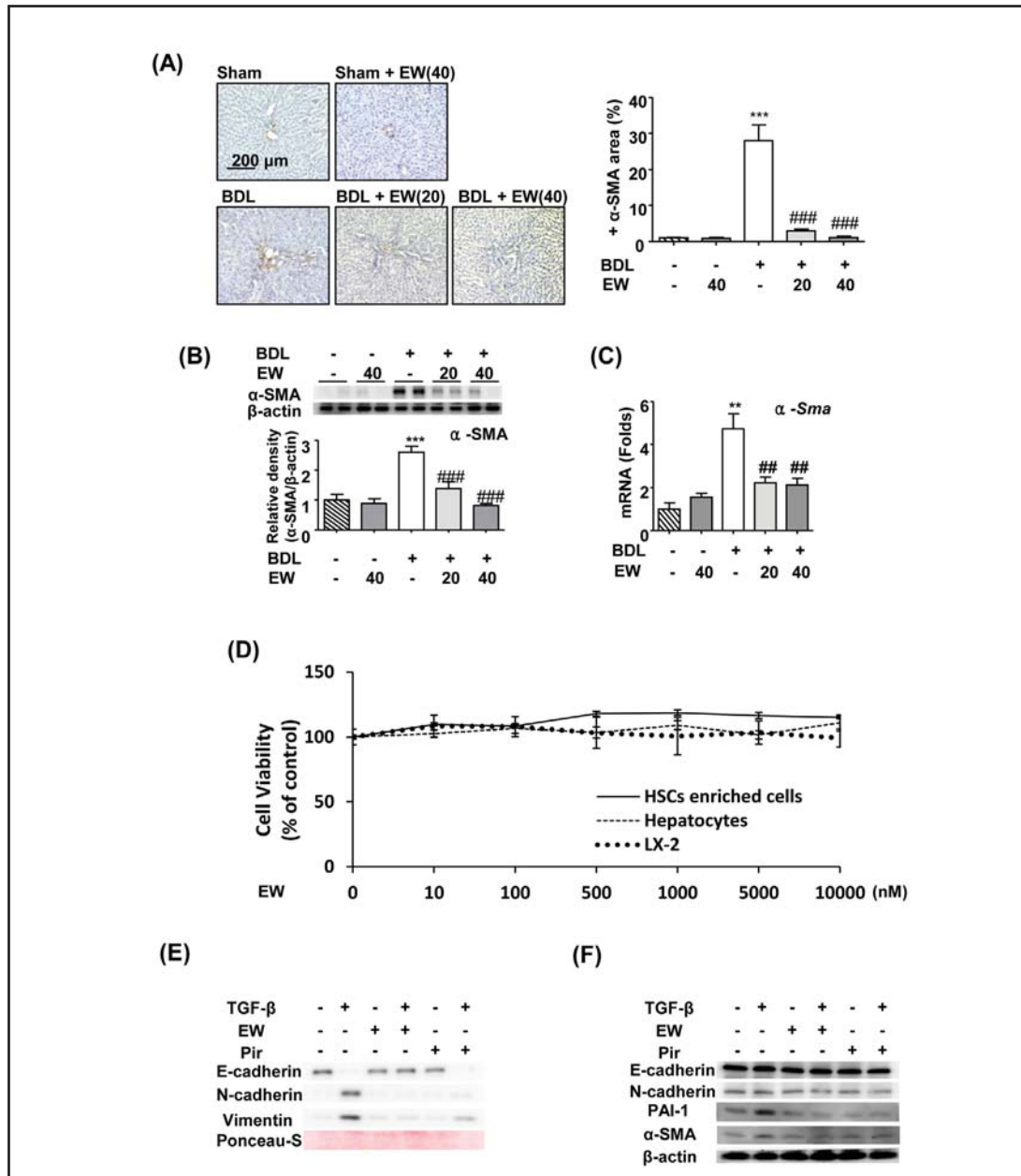
Cellular Physiology and Biochemistry

Cell Physiol Biochem 2016;38:571-588

DOI: 10.1159/000438651
Published online: February 05, 2016

© 2016 The Author(s). Published by S. Karger AG, Basel
www.karger.com/cpb

579

Kim et al.: EW-7197 Suppresses Cholestatic Liver Fibrosis

Fig. 3. EW-7197 inhibits HSC activation and EMT. (A) IHC (left) and densitometric analysis (right) of α-SMA staining of liver tissue from BDL rats. (B) Representative western blot images of α-SMA protein in liver tissue from BDL rats (top). Quantitative analysis of the relative density of α-SMA protein after normalization to β-actin (bottom). (C) Effects of EW-7197 on α-SMA (*α-Sma*) mRNA levels in liver tissue from BDL rats. *β-Actin* was used as a reference. (D) Effect of EW-7197 on proliferation of isolated primary hepatocytes, HSC-enriched cells, and LX-2 cells. Cells were seeded at a density of 5×10^3 cells per well in 96-well plates and treated with EW-7197 at concentrations of 10 nM to 10 μM for 72 h. Next, CCK-8 solution (10 μL) was added to each well, after which the plates were incubated for 1 h at 37 °C. Absorbance was measured at 450 nm with an ELISA microplate reader. (E) Effects of EW-7197 and pirfenidone (Pir) on E-cadherin, N-cadherin, and vimentin protein expression in isolated primary mouse HSC-enriched cells. Cells were treated with 0.5 μM of the indicated drug with or without TGF-β1 (2 ng/mL) and maintained for 24 h. Ponceau-S was used as a reference. (F) Effects of EW-7197 and Pir on E-cadherin, N-cadherin, PAI-I, and α-SMA protein expression in isolated primary mouse hepatocytes. Cells were treated with 0.5 μM of the indicated drug with or without TGF-β1 (2 ng/mL) and maintained for 24 h. β-actin was used as a reference.

Cellular Physiology and Biochemistry

Cell Physiol Biochem 2016;38:571-588

DOI: 10.1159/000438651
Published online: February 05, 2016

© 2016 The Author(s). Published by S. Karger AG, Basel
www.karger.com/cpb

580

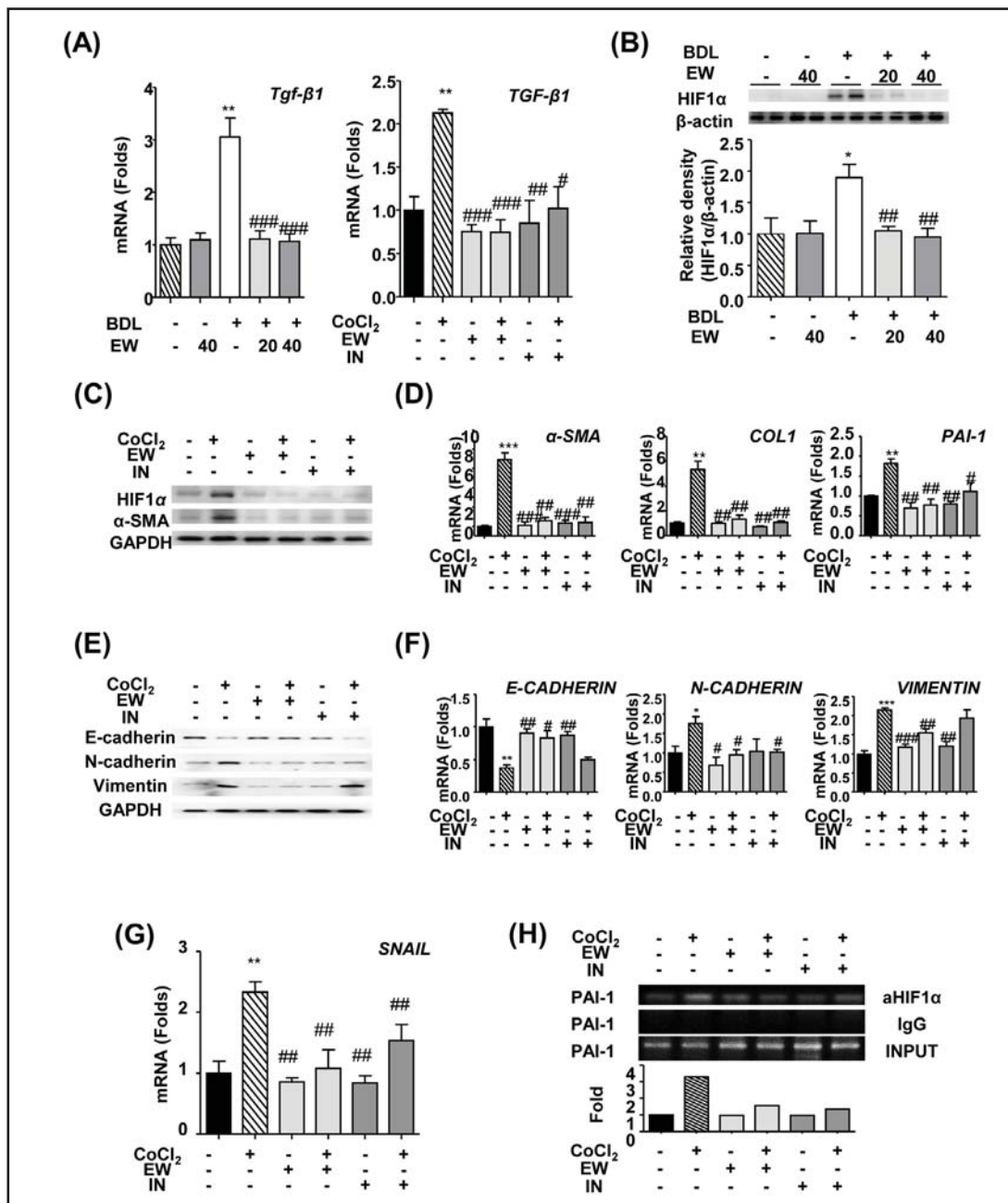Kim et al.: EW-7197 Suppresses Cholestatic Liver Fibrosis

Fig. 4. EW-7197 suppressed HIF1α-mediated HSC activation and the EMT. (A) Effect of EW-7197 on BDL-induced TGF-β mRNA levels. Real-time PCR analysis was performed as described in the methods section. TGF-β mRNA levels in BDL rats were downregulated by EW-7197. *β-Actin* was used as a reference. **$p < 0.01$ vs. sham and ###$p < 0.001$ vs. BDL (left). Effects of EW-7197 and IN-2001 on HIF1α-induced TGF-β mRNA levels in LX-2 cells. *PPIA* was used as a reference. *$p < 0.05$ vs. untreated control, **$p < 0.01$ vs. untreated control, ***$p < 0.001$ vs. untreated control, #$p < 0.05$ vs. $CoCl_2$-treated control, ##$p < 0.01$ vs. $CoCl_2$-treated control, ###$p < 0.001$ vs. $CoCl_2$-treated control (right). (B) Effects of EW-7197 on HIF1α protein expression in BDL rat livers. *$p < 0.05$ vs. sham, ***$p < 0.001$ vs. sham, ##$p < 0.01$ vs. BDL. (C) Effects of EW-7197 and IN-2001 on HIF1α and α-SMA expression in LX-2 cells. LX-2 cells were treated with 50 nM of the indicated drug with or without 100 μM $CoCl_2$ and maintained for 18 h. GAPDH was used as a reference. (D) Effects of EW-7197 and IN-2001 on α-SMA (*α-SMA*), collagen type 1 (*COl-1a1*), and PAI-1 (*PAI-1*) mRNA levels in LX-2 cells. *PPIA* was used as a reference. (E) Effects of EW-7197 and IN-2001 on E-cadherin, N-cadherin, and vimentin protein expression in LX-2 cells. GAPDH was used as a reference. (F) Effects of EW-7197 on E-cadherin (*CDH1*),

Cellular Physiology and Biochemistry

Cell Physiol Biochem 2016;38:571-588

DOI: 10.1159/000438651
Published online: February 05, 2016

© 2016 The Author(s). Published by S. Karger AG, Basel
www.karger.com/cpb

581

Kim et al.: EW-7197 Suppresses Cholestatic Liver Fibrosis

N-cadherin (*CDH2*), and vimentin (*VIM*) mRNA levels in LX-2 cells. *PPIA* was used as a reference. (G) Effects of EW-7197 and IN-2001 on *SNAIL* mRNA expression in LX-2 cells. LX-2 cells were treated with 50 nM of the indicated drug with or without 100 µM $CoCl_2$ and maintained for 18 h. *PPIA* was used as a reference. (H) Effects of EW-7197 and IN-2001 on promoter activation of PAI-1 as determined by ChIP assay. LX-2 cells were pretreated with 50 nM of the indicated drug for 30 min prior to the addition of 100 µM $CoCl_2$ and maintained for 3 h. ChIP assays were conducted at the PAI-1 promoter from LX-2 cells after immunoprecipitation with HIF1α antibodies. Densitometric analysis of (bottom) revealed the band intensity.

3E) in response to TGF-β. In contrast, primary mouse hepatocytes did not undergo EMT in response to TGF-β, which did not affect expression levels of E-cadherin or N-cadherin in these cells (Fig. 3F). Taken together, these results show that HSCs are highly responsive to TGF-β, which induces transformation of HSCs into myofibroblasts showing an EMT-like phenotype. Therefore, we focused on HSCs, rather than hepatocytes, in experiments intended to reveal the therapeutic mechanisms of ALK5 inhibitors in cholestatic liver fibrosis.

EW-7197 suppressed HIF1α-mediated HSC activation and the EMT

Hypoxia and elevated expression of HIF1α are typical phenomena observed in patients with obstructive cholestatic liver injury [38]. Because HIF1α is a key regulator of gene expression in response to hypoxia [39], we measured mRNA levels of TGF-β in BDL rats and LX-2 cells in order to gain insight into the role of cholestatic injury-mediated HIF1α induction in fibrosis and the inhibitory effect of EW-7197 on such induction. TGF-β mRNA levels were increased in BDL rats and $CoCl_2$-treated LX-2 cells (Fig. 4A); however, EW-7197 treatment reduced TGF-β mRNA levels *in vivo* and *in vitro*. Because we expected EW-7197 to produce its effects via the same mechanism in LX-2 cells and BDL rats, we used a lower dose (50 nM) of EW-7197 in comparison with that used in our previous study (0.5 µM). Because EW-7197 has a relatively low IC_{50}, the concentration used in this work should have resulted in 85% inhibition of ALK5 [40]. $CoCl_2$ is used to stabilize HIF1α, mimicking hypoxia [41]. Hypoxic conditions induce transcriptional activation of histone deacetylases (HDACs) *in vitro*, which downregulate expression of p53 and pVHL, leading to HIF1α activation [42]. Therefore, we compared the inhibitory effect of potent HDAC inhibitor IN-2001 on HIF1α expression with that of EW-7197. The effect of EW-7197 on HIF1α expression was assessed in BDL rats. EW-7197 inhibited elevation of HIF1α protein levels induced by cholestatic liver injury in BDL rats (Fig. 4B). To investigate the mechanism underlying hypoxia-dependent liver fibrosis, we measured HIF1α-induced activation of HSCs. In LX-2 cells, HIF1α and α-SMA protein levels were increased by $CoCl_2$ and reduced by treatment with EW-7197 or IN-2001 (Fig. 4C). Moreover, EW-7197 and IN-2001 decreased $CoCl_2$-induced α-SMA, Col1a, and PAI1 mRNA levels in LX-2 cells (Fig. 4D). To further examine the molecular mechanism of HIF1α-induced liver fibrosis, we examined the EMT in LX-2 cells. Expression of E-cadherin was not evident in LX-2 cells, whereas N-cadherin and vimentin increased in response to $CoCl_2$-induced hypoxic conditions. EW-7197 restored the protein and mRNA levels of E-cadherin and reduced those of N-cadherin and vimentin in $CoCl_2$-treated LX-2 cells. However, IN-2001 was not as potent as EW-7197 in $CoCl_2$-treated LX-2 cells (Fig. 4E and 4F). mRNA levels of Snail in $CoCl_2$-treated LX-2 cells are shown in Fig. 4G. Snail expression was increased by $CoCl_2$ and inhibited by EW-7197. To verify the effects of EW-7197 on HIF1α-induced transcription of plasminogen activator inhibitor-1 (PAI-1), a critical regulator of fibrosis, we performed ChIP assays in LX-2 cells. EW-7197 inhibited transactivation of HIF1α at the promoter region of PAI-1 (Fig. 4H). These data suggest that EW-7197 inhibits HIF1α-induced EMT, HSC activation, and ECM accumulation.

EW-7197 attenuates HIF1α-mediated oxidative stress in BDL rats and LX-2 cells

To determine whether oxidative stress was induced in the livers of BDL rats by hypoxia, we measured the expression of carbonic anhydrase IX (CAIX) and glucose transporter-1 protein (GLUT1) as intrinsic hypoxia markers [43-45]. The CAIX- and GLUT1-positive areas
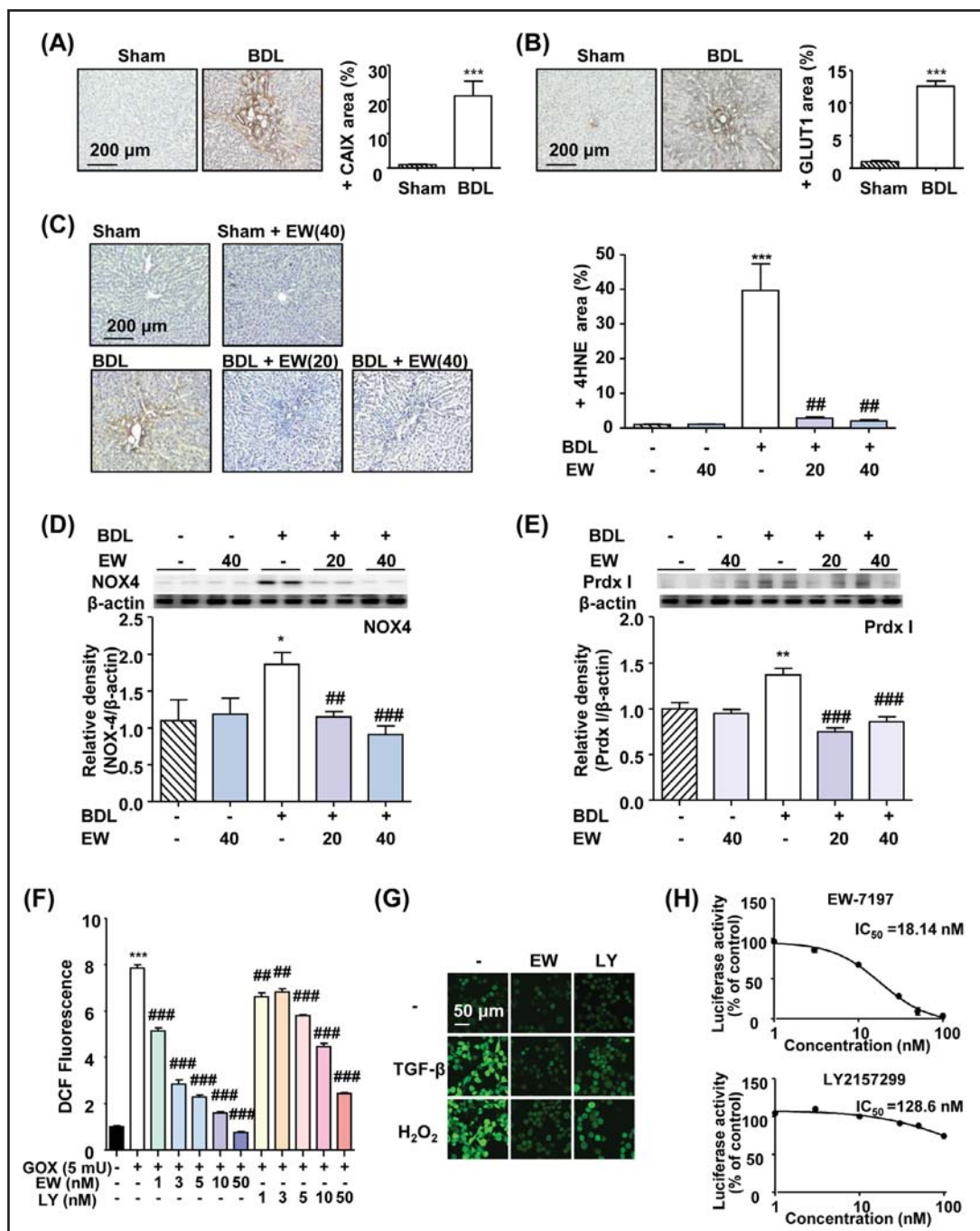
Cellular Physiology and Biochemistry

Cell Physiol Biochem 2016;38:571-588

DOI: 10.1159/000438651
Published online: February 05, 2016

© 2016 The Author(s). Published by S. Karger AG, Basel
www.karger.com/cpb

582

Kim et al.: EW-7197 Suppresses Cholestatic Liver Fibrosis

Fig. 5. EW-7197 attenuates HIF1α-mediated oxidative stress. (A) IHC of CAIX (top) and (B) GLUT1 (bottom). Densitometric analysis of CAIX (upper right) and GLUT1 (lower right) staining in liver tissue from BDL rats. (C) IHC of 4-hydroxynonenal (4HNE) (top) and densitometric analysis (bottom) of 4HNE staining in liver tissue from BDL rats. $^{***}p < 0.001$ vs. sham and $^{\#\#}p < 0.01$ vs. BDL. (D) Effect of EW-7197 on NOX4 protein expression in BDL rat livers. $^{*}p < 0.05$ vs. sham, $^{\#\#}p < 0.01$ vs. BDL, and $^{\#\#\#}p < 0.001$ vs. BDL. (E) Effects of EW-7197 on peroxiredoxin I (Prdx I) protein expression in BDL rat livers. $^{**}p < 0.01$ vs. sham and $^{\#\#\#}p < 0.001$ vs. BDL. (F) Effects of EW-7197 and LY2157299 on intracellular ROS generation induced by GOX (5 mU) for 18 h in LX-2 cells. Cells were treated with the indicated concentration of the drug in the presence of GOX (5 mU); $^{***}p < 0.001$ vs. control, $^{\#\#}p < 0.01$ vs. GOX, and $^{\#\#\#}p < 0.001$ vs. GOX. (G) Effects of EW-7197 and LY2157299 on 3TP-Lux promoter activity induced by TGF-β in HaCaT (3TP-Lux stable) cells. Cells were treated with the indicated concentration of the drug in the presence of TGF-β (2 ng/mL) for 24 h.

Cellular Physiology and Biochemistry

Cell Physiol Biochem 2016;38:571-588

DOI: 10.1159/000438651
Published online: February 05, 2016

© 2016 The Author(s). Published by S. Karger AG, Basel
www.karger.com/cpb

583

Kim et al.: EW-7197 Suppresses Cholestatic Liver Fibrosis

increased in size by 21.14-fold and 12.54-fold, respectively, in BDL rat livers in comparison with those of sham rats (Fig. 5A and 5B). These results indicate that hypoxia was induced in the livers of BDL rats by the BDL procedure, because oxidative stress occurs downstream of hypoxia-mediated signal transduction [46, 47]. In Fig. 5C, we showed the expression of 4-hydroxynonenal (4HNE), a marker of lipid peroxidation and oxidative stress. IHC staining showed a dramatic increase in the size of the 4HNE-positive area around the portal triad of the livers of BDL rats; however, EW-7197 treatment decreased the size of the 4HNE-positive area. These results show that oxidative stress was elevated in accordance with the increase in the size of the hypoxic area in the livers of BDL rats. A previous report showed that NADPH oxidase (NOX) was expressed in activated HSCs, in which it generated ROS that mediated fibrogenesis [48]. Western blot analysis showed that EW-7197 treatment inhibited the increase in NOX4 expression produced in rats by BDL (Fig. 5D). We also found that expression of antioxidant peroxiredoxin I (Prdx I) was elevated in BDL rats, while EW-7197 reduced the protein level of Prdx I (Fig. 5E). To investigate the inhibitory effect of EW-7197 on ROS generation, we performed an *in vitro* ROS assay in LX-2 cells. Administration of H_2O_2 or TGF-β to LX-2 cells increased the fluorescence of DCF which was inhibited by concomitant treatment with ALK5 inhibitors (Fig. 5F). Treatment of GOX that generates H_2O_2 to LX-2 cells increased fluorescence of DCF, which responds to ROS, by 8-fold however, treatment of GOX+EW-7197 and GOX+LY2157299 attenuated GOX-induced ROS generation in a dose-dependent manner. We used LY2157299 as a reference ALK5 inhibitor (Fig. 5G). The IC_{50} values of selected ALK5 inhibitors were determined by luciferase reporter gene assay in HaCaT (3TP-Lux stable) cells (Fig. 5H). The IC_{50} of EW-7197 (18.14 nM) was lower than that of LY2157299 (128.6 nM), indicating that EW-7197 was a more potent inhibitor of ALK5. These results indicate that ALK5 inhibitor EW-7197 inhibits ROS generation induced by cholestatic liver injuries with high potency *in vivo*.

EW-7197 inhibits liver fibrosis by blocking TGF-β/Smad signaling

In order to understand the fibrotic mechanism of TGF-β and inhibitory effect of EW-7197, we conducted immunofluorescence (IF) staining to visualize nuclear translocation of p-Smad2/3 (Fig. 6A). EW-7197 inhibited TGF-β-induced nuclear translocation of pSmad2/3 in LX-2 cells. EW-7197 inhibited protein and mRNA expression of TGF-β-stimulated EMT markers E-cadherin, N-cadherin, and vimentin in LX-2 cells (Fig. 6B and 6C). Moreover, TGF-β increased the mRNA level of Snail, whereas treatment with EW-7197 decreased Snail mRNA expression (Fig. 6D). These results demonstrate that TGF-β-induced EMT was involved in regulation of Snail. In addition, these data show that EW-7197 inhibits EMT induced by TGF-β-mediated Snail activation. Western blot and qRT-PCR analyses showed that EW-7197 inhibited TGF-β-induced α-SMA, Col1a, and PAI-1 protein and mRNA levels in LX-2 cells (Fig. 6E and 6F). Regulation of the expression of PAI-1, a profibrotic and TGF-β-responsive target gene, was mediated by Smad activation through ALK5 [24]. ChIP assays showed that EW-7197 inhibited transactivation of Smad2/3 at the promoter region of PAI-1 (Fig. 6G). Taken together, these results suggest that EW-7197 attenuates fibrosis via suppression of TGF-β-mediated HIF1α action, which ordinarily leads to HSC activation and the EMT (Fig. 6H).

Discussion

Liver fibrosis is a wound healing process that results in increased levels of ECM proteins [1, 32]. The pathogenesis of fibrosis involves TGF-β and hypoxia, which result in inflammation, activating quiescent HSCs and inducing their transformation into myofibroblasts [1, 32]. Following injury, vascular damage results in hypoxic conditions that lead to ROS generation [11], which might act as a mediator to bring about the EMT [12, 47, 49]. Cells respond to hypoxia by activating transcription factors, particularly HIF1α [13, 47]. HIF1α transcriptionally regulates the expression levels of ECM proteins (e.g., fibronectin and collagen), adhesion proteins (e.g., integrin), metabolic proteins (e.g., CAIX and GLUT1),
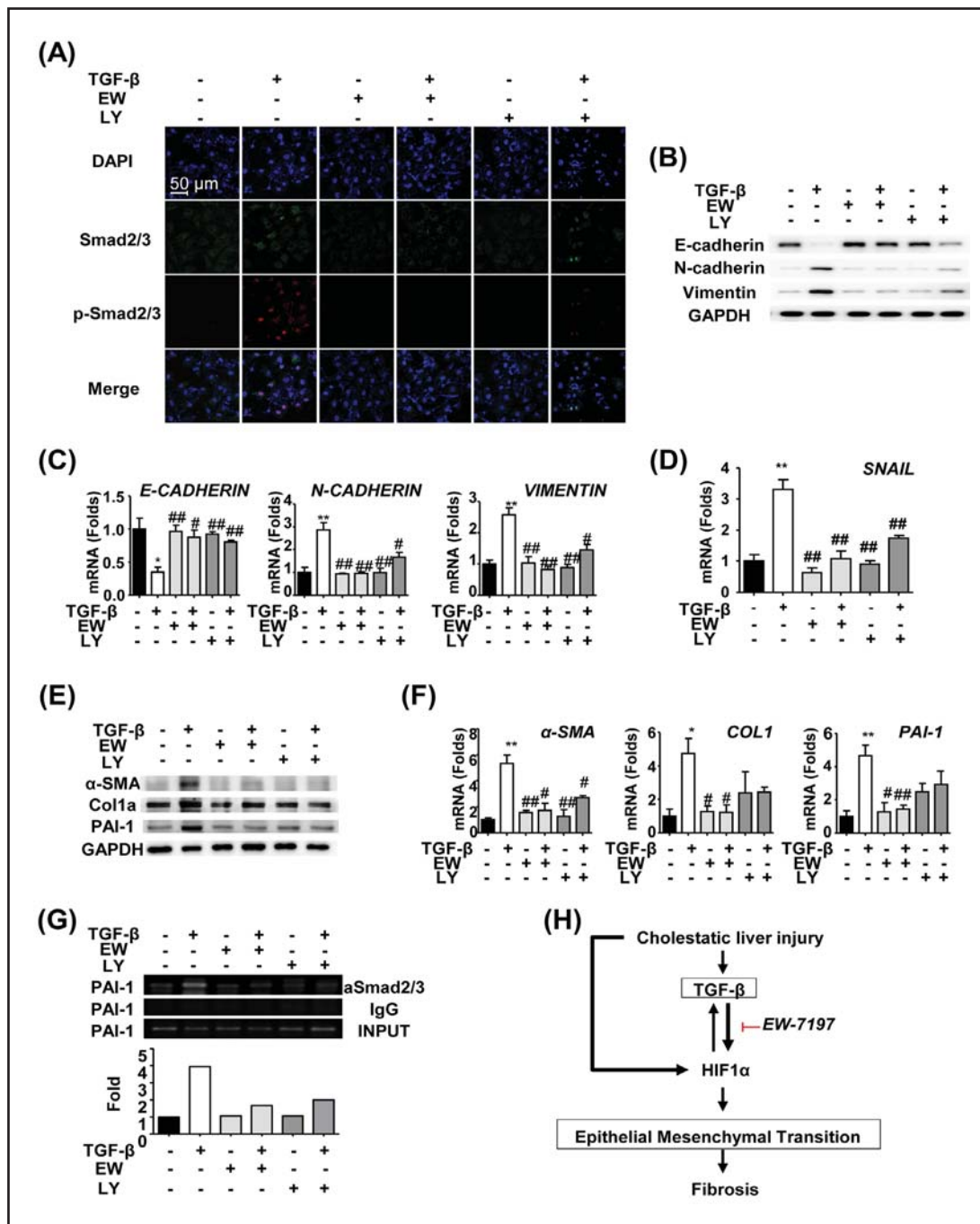
KARGER

Cellular Physiology and Biochemistry

Cell Physiol Biochem 2016;38:571-588

DOI: 10.1159/000438651
Published online: February 05, 2016

© 2016 The Author(s). Published by S. Karger AG, Basel
www.karger.com/cpb

584

Kim et al.: EW-7197 Suppresses Cholestatic Liver Fibrosis

Fig. 6. EW-7197 inhibits liver fibrosis by blocking TGF-β/Smad signaling. (A) Effects of EW-7197 on nuclear translocation of Smad2/3 and p-Smad2/3 in LX-2 cells. LX-2 cells were pretreated with 50 nM of the indicated drug for 30 min prior to the addition of TGF-β1 (2 ng/mL) and maintained for 30 min. Smad2/3, p-Smad2/3, and nuclei were stained with Alexa 488 (green), Alexa 555 (red), and DAPI (blue), respectively, after which the confocal images were merged (n > 3). The merged image reveals nuclear localization of p-Smad2/3 (pink). The scale bars are 50 μm. (B) Effects of EW-7197 and LY2157299 on E-cadherin, N-cadherin, and vimentin protein expression in LX-2 cells. LX-2 cells were treated with 50 nM of the indicated drug with or without TGF-β1 (2 ng/mL) and maintained for 24 h. β-actin was used as a reference. (C) Effects of EW-7197 and LY2157299 on E-cadherin (*CDH1*), N-cadherin (*CDH2*), and vimentin (*VIM*) mRNA levels in LX-2 cells. *PPIA* was used as a reference. (D) Effects of EW-7197 or LY2157299 on *SNAIL* mRNA expression in LX-2 cells. LX-2 cells were treated with 50 nM of the indicated drug with or without 2 ng/mL TGF-β and

Cellular Physiology and Biochemistry

Cell Physiol Biochem 2016;38:571-588

| DOI: 10.1159/000438651 | © 2016 The Author(s). Published by S. Karger AG, Basel |
| Published online: February 05, 2016 | www.karger.com/cpb |

Kim et al.: EW-7197 Suppresses Cholestatic Liver Fibrosis

585

maintained for 24 h. *PPIA* was used as a reference. **$p < 0.01$ vs. untreated control and ##$p < 0.01$ vs.TGF-β–treated control. (E) Effects of EW-7197 and LY2157299 on α-SMA, Col1a, and PAI-1 protein expression in LX-2 cells. LX-2 cells were treated with 50 nM of the indicated drug with or without TGF-β1 (2 ng/mL) and maintained for 24 h. GAPDH was used as a reference. (F) Effects of EW-7197 and LY2157299 on α-SMA (*α-SMA*), collagen type 1 (*COl-1a1*), and PAI-1(*PAI-1*) mRNA levels in LX-2 cells. *PPIA* was used as a reference. (G) Effects of EW-7197 and LY2157299 on promoter activation of PAI-1 as determined by ChIP assay. LX-2 cells were pretreated with 50 nM of the indicated drug for 30 min prior to the addition of TGF-β1 (2 ng/mL) and maintained for 30 min. ChIP assays were conducted at the PAI-1 promoter in LX-2 cells after immunoprecipitation with the Smad2/3 antibody. Densitometric analysis of the ChIP assay (down) revealed the band intensity after electrophoresis. (H) Simplified scheme revealing the effects of EW-7197 on TGF-β and HIF1α-induced EMT in cholestatic liver injury.

and growth factors (e.g., VEGF and TGF-β) [47]. TGF-β is modulated by HIF1α and is an effective mediator of the EMT and the progression of fibrosis in various organs [15, 20, 50, 51]. Activation of HSCs by TGF-β is an important event in tissue fibrogenesis, but activation of hepatocytes during the development of fibrosis in the mouse liver has not been observed [2]. Quiescent HSCs express epithelial marker E-cadherin and enter the EMT because of the actions of HIF1α and TGF-β [52-54]. These reports are in agreement with our results, in which only isolated mouse HSCs showed the EMT (Fig. 3 and 4). TGF-β and HIF1α are major cytokines that increase ROS generation and decrease concentrations of antioxidants during the progression of fibrosis [55-58]. In this paper we showed EW-7197 inhibited ROS generation by TGF-β or GOX (Fig. 5F and 5G) even though further study would be required to understand the mechanism of EW-7197. HIF1α increases expression levels of NOXs, which results in ROS generation [59, 60], regulating the transcriptional activity of HIF1α and driving the EMT [46, 61]. In addition, ROS generation induces Snail expression, subsequently leading to the EMT [62, 63] This study also showed that HIF1α increased ROS generation via NOX4 and demonstrated that ROS induced the EMT by inducing Snail expression in the livers of BDL rats and LX-2 cells (Fig. 5 and 6). Because TGF-β and HIF1α also play important roles in modulating inflammation related to liver fibrosis [64, 65], we showed that EW-7197 decreased the elevated level of NFκB expression in the livers of BDL rats (data not shown). However, further research is necessary to explain the manner in which TGF-β inhibition modulates the process of cholestatic fibrosis in terms of inflammation. Taken together, our results demonstrate that TGF-β inhibitor EW-7197 (20 and 40 mg/kg, po, *in vivo*) inhibited fibrosis by attenuating HIF1α-induced EMT in BDL rats.

Acknowledgements

Disclosure Statement

The authors state that they have no conflicts of interest.

References

1   Bataller R, Brenner DA: Liver fibrosis. J Clin Invest 2005;115:209.
2   Friedman SL: Molecular regulation of hepatic fibrosis, an integrated cellular response to tissue injury. J Biol Chem 2000;275:2247-2250.

KARGER

Cellular Physiology and Biochemistry

Cell Physiol Biochem 2016;38:571-588

DOI: 10.1159/000438651
Published online: February 05, 2016

© 2016 The Author(s). Published by S. Karger AG, Basel
www.karger.com/cpb

586

Kim et al.: EW-7197 Suppresses Cholestatic Liver Fibrosis

3 Wei Y, Huang M, Liu X, Yuan Z, Peng Y, Huang Z, Duan X, Zhao T: Anti-fibrotic effect of plumbagin on ccl4-lesioned rats. Cell Physiol Biochem 2015;35:1599-1608.

4 Zhang X, Tan Z, Wang Y, Tang J, Jiang R, Hou J, Zhuo H, Wang X, Ji J, Qin X: Ptpro-associated hepatic stellate cell activation plays a critical role in liver fibrosis. Cell Physiol Biochem 2015;35:885-898.

5 López-Novoa JM, Nieto MA: Inflammation and emt: An alliance towards organ fibrosis and cancer progression. EMBO Mol Med 2009;1:303-314.

6 Copple BL, Roth RA, Ganey PE: Anticoagulation and inhibition of nitric oxide synthase influence hepatic hypoxia after monocrotaline exposure. Toxicology 2006;225:128-137.

7 Corpechot C, Barbu V, Wendum D, Kinnman N, Rey C, Poupon R, Housset C, Rosmorduc O: Hypoxia-induced vegf and collagen i expressions are associated with angiogenesis and fibrogenesis in experimental cirrhosis. Hepatology 2002;35:1010-1021.

8 Ji S, Lemasters JJ, Christenson V, Thurman RG: Periportal and pericentral pyridine nucleotide fluorescence from the surface of the perfused liver: Evaluation of the hypothesis that chronic treatment with ethanol produces pericentral hypoxia. Proc Natl Acad Sci USA 1982;79:5415-5419.

9 Rosmorduc O, Wendum D, Corpechot C, Galy B, Sebbagh N, Raleigh J, Housset C, Poupon R: Hepatocellular hypoxia-induced vascular endothelial growth factor expression and angiogenesis in experimental biliary cirrhosis. Am J Pathol 1999;155:1065-1073.

10 Moon J-O, Welch TP, Gonzalez FJ, Copple BL: Reduced liver fibrosis in hypoxia-inducible factor-1α-deficient mice. Am J Physiol Gastrointest Liver Physiol 2009;296:G582-G592.

11 Rosmorduc O, Housset C: Hypoxia: A link between fibrogenesis, angiogenesis, and carcinogenesis in liver disease: Semin Liver Dis 2010;30,:258-270.

12 Cannito S, Novo E, Compagnone A, di Bonzo LV, Busletta C, Zamara E, Paternostro C, Povero D, Bandino A, Bozzo F: Redox mechanisms switch on hypoxia-dependent epithelial–mesenchymal transition in cancer cells. Carcinogenesis 2008;29:2267-2278.

13 Wang GL, Jiang B-H, Rue EA, Semenza GL: Hypoxia-inducible factor 1 is a basic-helix-loop-helix-pas heterodimer regulated by cellular o2 tension. Proc Natl Acad Sci USA 1995;92:5510-5514.

14 Polyak K, Weinberg RA: Transitions between epithelial and mesenchymal states: Acquisition of malignant and stem cell traits. Nat Rev Cancer 2009;9:265-273.

15 Higgins DF, Kimura K, Bernhardt WM, Shrimanker N, Akai Y, Hohenstein B, Saito Y, Johnson RS, Kretzler M, Cohen CD: Hypoxia promotes fibrogenesis in vivo via hif-1 stimulation of epithelial-to-mesenchymal transition. The J Clin Invest 2007;117:3810.

16 Tian H, Huang P, Zhao Z, Tang W, Xia J: Hif-1α plays a role in the chemotactic migration of hepatocarcinoma cells through the modulation of cxcl6 expression. Cell Physiol Biochem 2014;34:1536-1546.

17 Wang B-F, Wang X-J, Kang H-F, Bai M-H, Guan H-T, Wang Z-W, Zan Y, Song L-Q, Min W-L, Lin S: Saikosaponin-d enhances radiosensitivity of hepatoma cells under hypoxic conditions by inhibiting hypoxia-inducible factor-1α. Cell Physiol Biochem 2014;33:37-51.

18 Shi Y-F, Fong C-C, Zhang Q, Cheung P-Y, Tzang C-H, Wu RS, Yang M: Hypoxia induces the activation of human hepatic stellate cells lx-2 through tgf-β signaling pathway. FEBS Lett 2007;581:203-210.

19 Meurer SK, Tihaa L, Borkham-Kamphorst E, Weiskirchen R: Expression and functional analysis of endoglin in isolated liver cells and its involvement in fibrogenic smad signalling. Cell Signal 2011;23:683-699.

20 Leask A, Abraham DJ: Tgf-β signaling and the fibrotic response. FASEB J 2004;18:816-827.

21 Falanga V, Qian VSW, Danielpour D, Katz MH, Roberts AB, Sporn MB: Hypoxia upregulates the synthesis of tgf-β1 by human dermal fibroblasts. J Invest Dermatol 1991;97:634-637.

22 Sheen YY, Kim M-J, Park S-A, Park S-Y, Nam J-S: Targeting the transforming growth factor-β signaling in cancer therapy. Biomol Ther (Seoul) 2013;21:323.

23 Kaimori A, Potter J, Kaimori J-y, Wang C, Mezey E, Koteish A: Transforming growth factor-β1 induces an epithelial-to-mesenchymal transition state in mouse hepatocytes in vitro. J Biol Chem 2007;282:22089-22101.

24 Verrecchia F, Mauviel A: Transforming growth factor-beta and fibrosis. World J Gastroenterol 2007;13:3056-3062.

25 Ikegami T, Zhang Y, Matsuzaki Y: Liver fibrosis: Possible involvement of emt. Cells Tissues Organs 2006;185:213-221.

26 Ji D, Li B, Shao Q, Li F, Li Z, Chen G: Mir-22 suppresses bmp7 in the development of cirrhosis. Cell Physiol Biochem 2015;36:1026-1036.

27   Gressner A, Weiskirchen R: Modern pathogenetic concepts of liver fibrosis suggest stellate cells and tgf-β as major players and therapeutic targets. J Cell Mol Med 2006;10:76-99.

28   Gouville AC, Boullay V, Krysa G, Pilot J, Brusq JM, Loriolle F, Gauthier JM, Papworth SA, Laroze A, Gellibert F: Inhibition of tgf-β signaling by an alk5 inhibitor protects rats from dimethylnitrosamine-induced liver fibrosis. Br J Pharmacol 2005;145:166-177.

29   Park S-A, Kim M-J, Park S-Y, Kim J-S, Lee S-J, Woo HA, Kim D-K, Nam J-S, Sheen YY: Ew-7197 inhibits hepatic, renal, and pulmonary fibrosis by blocking tgf-β/smad and ros signaling. Cell Mol Life Sci 2014:1-17.

30   Bergheim I, Guo L, Davis MA, Duveau I, Arteel GE: Critical role of plasminogen activator inhibitor-1 in cholestatic liver injury and fibrosis. J Pharmacol Exp Ther 2006;316:592-600.

31   Jin CH, Krishnaiah M, Sreenu D, Subrahmanyam VB, Rao KS, Lee HJ, Park S-J, Park H-J, Lee K, Sheen YY: Discovery of n-((4-([1, 2, 4] triazolo [1, 5-a] pyridin-6-yl)-5-(6-methylpyridin-2-yl)-1 h-imidazol-2-yl) methyl)-2-fluoroaniline (ew-7197): A highly potent, selective, and orally bioavailable inhibitor of tgf-β type i receptor kinase as cancer immunotherapeutic/antifibrotic agent. J Med Chem 2014;57:4213-4238.

32   Henderson N, Iredale J: Liver fibrosis: Cellular mechanisms of progression and resolution. Clin Sci 2007;112:265-280.

33   Xu J, Lamouille S, Derynck R: Tgf-β-induced epithelial to mesenchymal transition. Cell Res 2009;19:156-172.

34   Scheel C, Weinberg RA: Cancer stem cells and epithelial–mesenchymal transition: Concepts and molecular links: Semin Cancer Biol 2012;22:396-403.

35   Canbay A, Friedman S, Gores GJ: Apoptosis: The nexus of liver injury and fibrosis. Hepatology 2004;39:273-278.

36   Moreira RK: Hepatic stellate cells and liver fibrosis. Arch Pathol Lab Med. 2007;131:1728-1734.

37   Jia S, Liu X, Li W, Xie J, Yang L, Li L: Peroxisome proliferator-activated receptor gamma negatively regulates the differentiation of bone marrow-derived mesenchymal stem cells toward myofibroblasts in liver fibrogenesis. Cell Physiol Biochem 2015;37:2085-2100.

38   Nath B, Szabo G: Hypoxia and hypoxia inducible factors: Diverse roles in liver diseases. Hepatology 2012;55:622-633.

39   Semenza GL: Expression of hypoxia-inducible factor 1: Mechanisms and consequences. Biochem Pharmacol 2000;59:47-53.

40   Son JY, Park S-Y, Kim S-J, Lee SJ, Park S-A, Kim M-J, Kim SW, Kim D-K, Nam J-S, Sheen YY: Ew-7197, a novel alk-5 kinase inhibitor, potently inhibits breast to lung metastasis. Mol Cancer Ther 2014;13:1704-1716.

41   PIRET JP, Mottet D, Raes M, Michiels C: Cocl2, a chemical inducer of hypoxia-inducible factor-1, and hypoxia reduce apoptotic cell death in hepatoma cell line hepg2. Ann N Y Acad Sci 2002;973:443-447.

42   Liang D, Kong X, Sang N: Effects of histone deacetylase inhibitors on hif-1. Cell Cycle 2006;5:2430-2435.

43   Airley R, Loncaster J, Davidson S, Bromley M, Roberts S, Patterson A, Hunter R, Stratford I, West C: Glucose transporter glut-1 expression correlates with tumor hypoxia and predicts metastasis-free survival in advanced carcinoma of the cervix. Clin Cancer Res 2001;7:928-934.

44   Airley RE, Loncaster J, Raleigh JA, Harris AL, Davidson SE, Hunter RD, West CM, Stratford IJ: Glut-1 and caix as intrinsic markers of hypoxia in carcinoma of the cervix: Relationship to pimonidazole binding. Int J Cancer 2003;104:85-91.

45   Hoskin P, Sibtain A, Daley F, Wilson G: Glut1 and caix as intrinsic markers of hypoxia in bladder cancer: Relationship with vascularity and proliferation as predictors of outcome of arcon. Br J Cancer 2003;89:1290-1297.

46   Cannito S, Paternostro C, Busletta C, Bocca C, Colombatto S, Miglietta A, Novo E, Parola M: Hypoxia, hypoxia-inducible factors and fibrogenesis in chronic liver diseases. Histol Histopathol 2014;29:33-44.

47   Lokmic Z, Musyoka J, Hewitson TD, Darby IA: 3 hypoxia and hypoxia signaling in tissue repair and fibrosis. Int Rev Cell Mol Biol 2012;296:139.

48   Pellicoro A, Ramachandran P, Iredale JP, Fallowfield JA: Liver fibrosis and repair: Immune regulation of wound healing in a solid organ. Nat Rev Immunol 2014;14:181-194.

49   Higgins DF, Kimura K, Iwano M, Haase VH: Hypoxia-inducible factor signaling in the development of tissue fibrosis. Cell Cycle 2008;7:1128-1132.

50   Liu X, Hu H, Yin JQ: Therapeutic strategies against tgf-β signaling pathway in hepatic fibrosis. Liver Int 2006;26:8-22.

KARGER

Cellular Physiology and Biochemistry

Cell Physiol Biochem 2016;38:571-588

DOI: 10.1159/000438651

Published online: February 05, 2016

© 2016 The Author(s). Published by S. Karger AG, Basel
www.karger.com/cpb

588

Kim et al.: EW-7197 Suppresses Cholestatic Liver Fibrosis

51 Ueno M, Maeno T, Nomura M, Aoyagi-Ikeda K, Matsui H, Hara K, Tanaka T, Iso T, Suga T, Kurabayashi M: Hypoxia-inducible factor-1α mediates tgf-β-induced pai-1 production in alveolar macrophages in pulmonary fibrosis. Am J Physiol Lung Cell Mol Physiol 2011;300:L740-L752.

52 Lim Y-S, Lee HC, Lee H-S: Switch of cadherin expression from e-to n-type during the activation of rat hepatic stellate cells. Histochem Cell Biol 2007;127:149-160.

53 Sicklick JK, Choi SS, Bustamante M, McCall SJ, Pérez EH, Huang J, Li Y-X, Rojkind M, Diehl AM: Evidence for epithelial-mesenchymal transitions in adult liver cells. Am J Physiol Gastrointest Liver Physiol 2006;291:G575-G583.

54 Copple BL: Hypoxia stimulates hepatocyte epithelial to mesenchymal transition by hypoxia-inducible factor and transforming growth factor-β-dependent mechanisms. Liver Int 2010;30:669-682.

55 Prabhakar NR, Kumar GK, Nanduri J, Semenza GL: Ros signaling in systemic and cellular responses to chronic intermittent hypoxia. Antioxid Redox Sign 2007;9:1397-1404.

56 Hsieh H-L, Wang H-H, Wu W-B, Chu P-J, Yang C-M: Transforming growth factor-b1 induces matrix metalloproteinase-9 and cell migration in astrocytes: Roles of ros-dependent erk-and jnk-nf-kb pathways. J Neuroinflammation 2010;7:88.

57 Salles MB, Gehrke SA, Koo S, Allegrini Jr S, Rogero SO, Ikeda TI, Cruz ÁS, Shinohara EH, Yoshimoto M: An alternative to nerve repair using an antioxidant compound: A histological study in rats. J Mater Sci Mater Med 2015;26:1-8.

58 Rhee SG, Chae HZ, Kim K: Peroxiredoxins: A historical overview and speculative preview of novel mechanisms and emerging concepts in cell signaling. Free Radic Biol Med. 2005;38:1543-1552.

59 Yuan G, Khan SA, Luo W, Nanduri J, Semenza GL, Prabhakar NR: Hypoxia-inducible factor 1 mediates increased expression of nadph oxidase-2 in response to intermittent hypoxia. J Cell Physiol 2011;226:2925-2933.

60 Jiang F, Liu G-S, Dusting GJ, Chan EC: Nadph oxidase-dependent redox signaling in tgf-β-mediated fibrotic responses. Redox Biol 2014;2:267-272.

61 Pouysségur J, Mechta-Grigoriou F: Redox regulation of the hypoxia-inducible factor. Biol Chem 2006;387:1337-1346.

62 Park S-Y, Kim M-J, Park S-A, Kim J-S, Min K-N, Kim D-K, Lim W, Nam J-S, Sheen YY: Combinatorial tgf-β attenuation with paclitaxel inhibits the epithelial-to-mesenchymal transition and breast cancer stem-like cells. Oncotarget 2015;6:37526-37543.

63 Cichon MA, Radisky DC: Ros-induced epithelial-mesenchymal transition in mammary epithelial cells is mediated by nf-κb-dependent activation of snail. Oncotarget 2014;5:2827.

64 Xiao J, Ho CT, Liong EC, Nanji AA, Leung TM, Lau TYH, Fung ML, Tipoe GL: Epigallocatechin gallate attenuates fibrosis, oxidative stress, and inflammation in non-alcoholic fatty liver disease rat model through tgf/smad, pi3 k/akt/foxo1, and nf-kappa b pathways. Eur J Nutr 2014;53:187-199.

65 Sheppard D: Transforming growth factor β: A central modulator of pulmonary and airway inflammation and fibrosis. Proc Am Thorac Soc 2006;3:413-417.

KARGER

KARGER